HTML ABSTRACT + LINKS

APPLIED PHYSICS LETTERS VOLUME 85, NUMBER 10 6 SEPTEMBER 2004

Mechanisms of nitrogen incorporation in GaAsN alloys

M. Reason, H. A. McKay, W. Ye, S. Hanson, and R. S. Goldman[a)]
Department of Materials Science and Engineering, University of Michigan, Ann Arbor, Michigan 48109-2136

V. Rotberg
Department of Nuclear Engineering and Radiological Sciences, University of Michigan, Ann Arbor, Michigan 48109-2145

(Received 8 April 2004; accepted 6 July 2004)

We have investigated nitrogen incorporation mechanisms in dilute nitride GaAsN alloys grown by plasma-assisted molecular-beam epitaxy. A comparison of nuclear reaction analysis and Rutherford backscattering spectrometry in channeling and nonchanneling conditions reveals significant composition-dependent incorporation of N into nonsubstitutional sites, presumably as either N–N or N–As split interstitials. Furthermore, we identify the (2×1) reconstruction as the surface structure which leads to the highest substitutional N incorporation, likely due to the high number of group V sites per unit area available for N–As surface exchange. © *2004 American Institute of Physics*. [DOI: 10.1063/1.1789237]

For many III–V–N alloys, the band-gap energy is reduced as the nitrogen composition increases.[1–3] For example, for ~1% N added to GaAs, the band gap is reduced by ~200 meV.[2] The resulting dilute nitride semiconductors are promising for a wide range of applications including long-wavelength light-emitters, high-performance electronic devices, and high efficiency solar cells. For GaAsN alloys, the electron mobility and optical emission intensity decrease as the nitrogen incorporation increases.[4–6] However, conflicting results have been reported regarding the mechanism of N incorporation in GaAsN,[7–11] and the relationship between the mechanism of N incorporation and the GaAsN surface reconstruction has not been reported.

Ahlgren *et al.*[7] observed a nearly constant interstitial N concentration of 2×10^{19} cm^{-3} for 100 nm thick films with total N concentrations ranging from 1.8 to 9.7×10^{20} cm^{-3}. Bisognin *et al.*[8] reported N contamination of 2×10^{14} cm^{-2} on the surface of a series of 150 nm thick GaAsN films with total N concentrations ranging from 3.8 to 10×10^{20} cm^{-3}. They reasoned that the apparent interstitial N measured by Ahlgren *et al.* was likely caused by a similar N surface contamination, which would be consistent with the first-principles total-energy calculations prediction of an interstitial N concentration of $\sim1\times10^{14}$ cm^{-3}.[9] On the other hand, Spruytte *et al.*[10] reported a much larger interstitial N concentration of 1.5×10^{20} cm^{-3} for one 200 nm sample with total N concentration of 7×10^{20} cm^{-3}, likely not entirely accounted for by N surface contamination. The potential artifact of N surface contamination may be further minimized for even thicker films. To date, Alt *et al.*[11] have reported an interstitial concentration of $\sim6\times10^{18}$ cm^{-3} in one 350 nm thick GaAsN film with total N concentration of 1.3×10^{20} cm^{-3}. We report significant composition-dependent interstitial N incorporation in 500 nm thick GaAsN films with total N concentration ranging from 1.5 to 8.5×10^{20} cm^{-3}. We identify the (2×1) reconstruction as the surface structure which leads to the highest substitutional N incorporation, likely due to the high number of group V sites per unit area available for N–As exchange.

The $GaAs_{1-x}N_x$ alloy films were grown on epiready (001) GaAs by molecular-beam epitaxy (MBE), using solid Ga and As_4 or As_2, and a radio frequency (rf) plasma source, with ultrahigh purity 10% N_2/Ar. The N composition in the $GaAs_{1-x}N_x$ layers, x, was adjusted by varying the GaAs growth rate between 0.25 and 1.2 μm/h.[10] The surface reconstruction was monitored *in situ* with reflection high-energy electron diffraction (RHEED). The substrate temperature was monitored using an optical pyrometer, calibrated to the (2×4)–(3×1) and (3×1)–(4×2) surface reconstruction changes at 500 and 595 °C, respectively.[12]

GaAs substrates were mounted either on In-bonded or In-free molybdenum blocks. Each sample contained an initial 500 nm GaAs buffer layer grown at 580 °C. For some samples, the substrate temperature was lowered to 500 °C, and an additional 20 nm layer of GaAs was grown.[13] For other samples, a series of annealing steps was performed at 580 and 530 °C with As overpressure, followed by a 370 °C anneal without As.[14] Finally, ~500 nm thick $GaAs_{1-x}N_x$ layers with x ranging from 0.005 to 0.035 were grown at 400, 550, or 580 °C. All the $GaAs_{1-x}N_x$ layers were grown with a high As/Ga beam-equivalent pressure ratio (>30 for As_4 and ~20 for As_2). Some of the samples were subsequently annealed at the GaAsN growth temperature with As overpressure, followed by a 370 °C anneal without As.

Figure 1 shows the RHEED patterns collected during the growth of the 580 °C GaAs buffer layer, and the GaAsN layers at 400, 550, and 580 °C. During the growth of the 580 °C buffer layer, RHEED reveals a streaky (2×4) pattern, shown in Figs. 1(a) and 1(b). For the GaAsN layers grown at 400 °C, the intensity of the center streak of the $(2\times)$ pattern is reduced, and a streaky (2×1) pattern is evident, as shown in Figs. 1(c) and 1(d). For GaAsN layers grown at 550 °C, the center streak of the $(2\times)$ pattern transforms to two streaks, and a slightly spotty (3×1) pattern is evident, as shown in Figs. 1(e) and 1(f). Finally, for GaAsN layers grown at 580 °C, the RHEED pattern is essentially identical to that shown for the GaAs buffer layer in Figs. 1(a)

[a)]Author to whom correspondence should be addressed; electronic mail: rsgold@umich.edu

 © 2004 American Institute of Physics

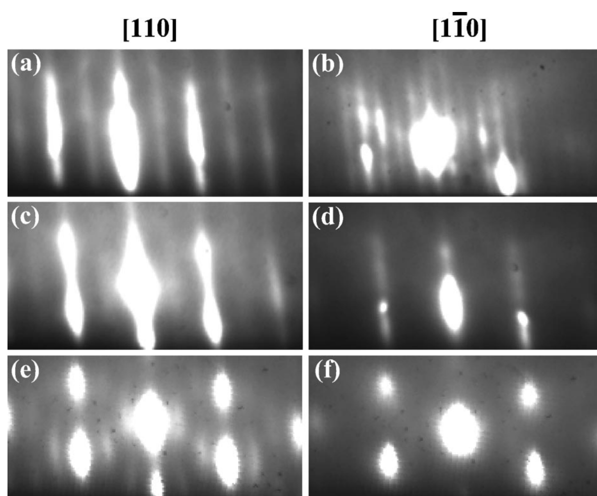

FIG. 1. RHEED patterns collected along the [110] and [1$\bar{1}$0] axes during growth of (a) and (b) GaAs buffer layer grown at 580 °C, and GaAsN films at (c) 400 °C, (d) 400 °C, (e) 550 °C, and (f) 550 °C. GaAsN grown at 580 °C was essentially identical to (a) and (b).

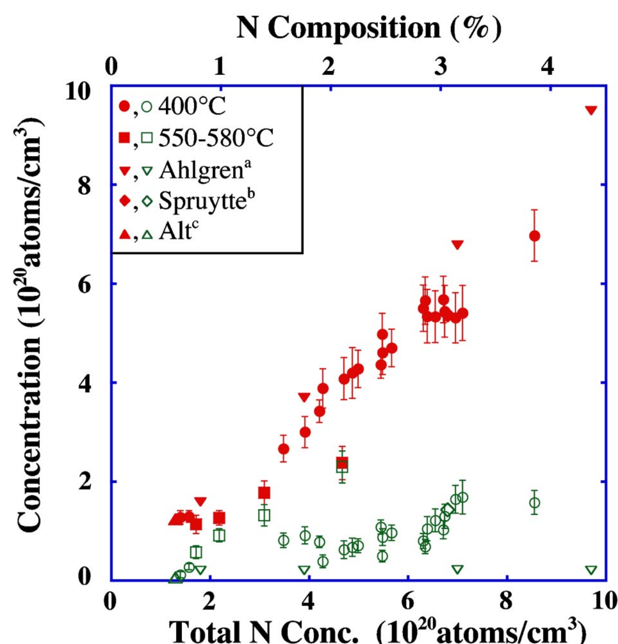

FIG. 2. (Color online) Substitutional (solid symbols) and interstitial (open symbols) concentrations vs. total N concentration for $GaAs_{1-x}N_x$ films with varying x. The concentration of interstitial N increases with total N concentation. [a]See Ref. 7. [b]See Ref. 10. [c]See Ref. 11.

and 1(b). These surface reconstructions are consistent with reports of GaAsN growth.[15–17] The surface morphology of the films was examined *ex situ* with tapping mode atomic force microscopy (AFM). For GaAsN films grown at 400 °C, the rms roughness was 0.3±0.1 nm, similar to that of the GaAs buffer layer. Meanwhile, for GaAsN films grown in the range of 550–580 °C, the rms roughness increased to 1.3±0.1 nm.

The total N concentration and fraction of N incorporated substitutionally, f, were determined using nuclear reaction analysis (NRA) with the $^{14}N(d,\alpha_0)^{12}C$ and $^{14}N(d,\alpha_1)^{12}C$ reactions. We used 1.4 MeV deuterons, which have a penetration depth of ~15 μm, much greater than the thickness of the GaAsN films.[18] The emitted α_0 and α_1 particles were collected using a detector with a solid angle of 5 msr, at a scattering angle of 150°, for which the scattering cross section is well known.[19] The N concentrations determined using the yields from α_0 and α_1 particles were within 6%, less than the average measurement error. NRA measurements of GaAsN and Rutherford backscattering spectrometry (RBS) measurements of GaAs were performed in both [001] channeling conditions, and tilted ~5° away from the [001] axis, which we define as a "nonchanneling" condition. Multiple channeling and nonchanneling measurements performed on the same location revealed negligible lattice damage induced by the deuteron beam. To determine f, we assume stoichiometric undoped GaAs reference samples with negligible interstitial concentrations, typical of high temperature grown GaAs.[20] Furthermore, we assume homogeneous random GaAsN alloys, as suggested by prior scanning tunneling microscopy measurements of similar samples.[21] The fraction of N incorporating substitutionally is given by

$$f = \frac{1-\chi(\mathrm{N})}{1-\chi_{\min}(\mathrm{GaAs})}, \tag{1}$$

where $\chi_{\min}$(GaAs) [χ(N)] is the ratio of the yield in channeling and nonchanneling conditions for GaAs [N]. For GaAs reference samples grown by MBE, $\chi_{\min}$ was 0.057±0.005, similar to earlier reports.[7] The χ(N) values ranged from 0.14±0.03 to 0.52±0.05 for a variety of GaAsN films.

Figure 2 shows a plot of substitutional and interstitial N concentrations as a function of the total N concentration for a variety of films. The plot reveals an increase in both substitutional and interstitial N concentrations as a function of total N concentration. For total N concentrations below 2×10^{20} cm^{-3}, we observe interstitial concentrations similar to Ahlgren *et al.*[7] and Alt *et al.*[11] However, for total N concentrations above 4×10^{20} cm^{-3}, we observe significantly greater interstitial concentrations than Ahlgren *et al.*[7] Instead, we observe interstitial N concentrations similar to Spruytte *et al.*[10] Since our films are 500 nm thick, N surface contamination of 2×10^{14} cm^{-2} would lead to 4×10^{18} cm^{-3} interstitial N concentration, less than 33% of our lowest interstitial N concentration. Thus, we expect that our significant interstitial N concentrations cannot be accounted for by N surface contamination. Interestingly, for GaAsN grown at 550 and 580 °C, with the (3×1) and (2×4) reconstructions, respectively, we observe substantially higher fractions of interstitial N than for GaAsN grown at 400 °C, with the (2×1) reconstruction. Since the (2×1) reconstructed surface has significantly more group V sites per unit area than the (3×1) or (2×4) surfaces,[22–24] N atoms may more effectively incorporate substitutionally via N–As exchange.[25] This change in the mechanism of N incorporation for high temperature GaAsN growth may contribute to the increase in surface roughness discussed earlier. A similar trend has been reported for nonsubstitutional C incorporation in SiGeC alloys.[26]

The interstitial concentrations shown in Fig. 2 indicate the number of N atoms in interstitial sites per unit volume, which may not be equivalent to the number of N interstitial defects per unit volume. Both calculations[9] and experiments[27] have suggested that the dominant form of interstitial N is either the N–As split interstitial, NAs_{split}, or the N–N split interstitial, NN_{split}, shown in Fig. 3. Our channeling measurements do not distinguish these forms of inter-

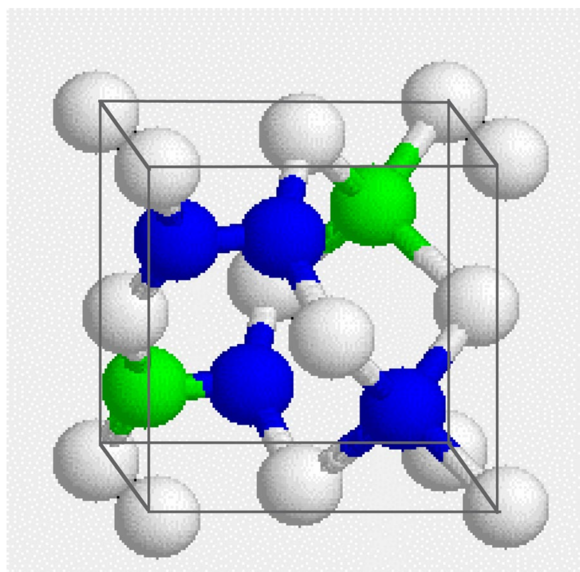

FIG. 3. (Color online) Ball and stick crystal schematic for GaAsN with substitutional N, N–As split interstitial, and N–N split interstitial. The white, grey (green), and black (blue) spheres represent Ga, As, and N, respectively.

stitial N. If NAs_{split} is dominant in GaAsN, the interstitial concentration would be equal to the concentration of N atoms in interstitial sites in Fig. 2. Alternatively, if NN_{split} is dominant in GaAsN, the interstitial concentration would be equal to half the concentration of N atoms in interstitial sites in Fig. 2. Deep level transient Fourier spectroscopy (DLTFS) measurements have suggested that NN_{split} and NAs_{split} are the dominant defects for $GaAs_{1-x}N_x$ with $x<0.1\%$ and $x=0.5\%$, respectively.[27] In order to determine the dominant defect for higher N compositions, further DLTFS experiments are needed.

In summary, we have investigated nitrogen incorporation mechanisms in $GaAs_{1-x}N_x$ films using a combination of *in situ* RHEED and *ex situ* AFM, NRA, and RBS. A comparison of NRA and RBS in channeling and nonchanneling conditions reveals significant composition-dependent nonsubstitutional N, which cannot be accounted for by N surface contamination. Furthermore, growth of GaAsN films at $400°C$, with a (2×1) surface reconstruction, leads to the highest substitutional incorporation of N. This is likely due to the higher number of group V sites per unit area available on the (2×1) reconstructed surface in comparison with the (3×1) and (2×4) reconstructed surfaces.

This work was supported in part by the National Science Foundation Early Faculty CAREER, Instrumentation for Materials Research, and Nanoscale Exploratory Research Programs (Grant Nos. 9773707, 9975701, and 0210714); the DoD Multidisciplinary University Research Initiative administered by the Air Force Office of Scientific Research under Grant No. F49620-00-1-0328; the Department of Energy, through the National Renewable Energy Laboratory Photovoltaics Beyond the Horizon Program under Contract No. ACQ-1-30619-14; the TRW Foundation; and k-Space Associates, Inc. The authors acknowledge G.S. Was, S.-H. Wei, and A. Zunger for useful discussions, and the assistance of the staff of the Michigan Ion Beam Laboratory.

[1] M. Weyers, M. Sato, and H. Ando, Jpn. J. Appl. Phys., Part 1 **31**, 853 (1992).
[2] W. G. Bi and C. W. Tu, Appl. Phys. Lett. **70**, 1608 (1997).
[3] L. Bellaiche, S.-H. Wei, and A. Zunger, Phys. Rev. B **54**, 17568 (1996).
[4] R. Mouillet, L.-A. de Vaulchier, E. Deleporte, Y. Guldner, L. Travers, and J.-C. Harmand, Solid State Commun. **126**, 333 (2003).
[5] J. S. Wang, A. R. Kovsh, L. Wei, J. Y. Chi, Y. T. Wu, P. Y. Wang, and V. M. Ustinov, Nanotechnology **12**, 430 (2001).
[6] I. A. Buyanova, W. M. Chen, and C. W. Tu, Semicond. Sci. Technol. **17**, 815 (2002).
[7] T. Ahlgren, E. Vainonen-Ahlgren, J. Likonen, W. Li, and M. Pessa, Appl. Phys. Lett. **80**, 2314 (2002).
[8] G. Bisognin, D. De Salvador, C. Mattevi, M. Berti, A. V. Drigo, G. Ciatto, L. Grenouillet, P. Duvaut, P. Gilet, and H. Mariette, J. Appl. Phys. **95**, 48 (2004).
[9] S. B. Zhang and S.-H. Wei, Phys. Rev. Lett. **86**, 1789 (2001).
[10] S. G. Spruytte, M. C. Larson, W. Wampler, C. W. Coldren, H. E. Petersen, and J. S. Harris, J. Cryst. Growth **227-228**, 506 (2001).
[11] H. C. Alt, A. Y. Egorov, H. Riechert, J. D. Meyer, and B. Wiedemann, Physica B **308-310**, 877 (2001).
[12] H. Shtrikman (private communication).
[13] D. W. Gotthold, S. Govindaraju, T. Mattord, A. L. Holmes, Jr., and B. G. Streetman, J. Vac. Sci. Technol. A **18**, 461 (2000).
[14] B. D. Schultz, H. H. Farrell, M. M. R. Evans, K. Ludge, and C. J. Palmstrom, J. Vac. Sci. Technol. B **20**, 1600 (2002).
[15] M.-A. Pinault and E. Tournie, Appl. Phys. Lett. **79**, 3404 (2001).
[16] A. R. Kovsh, J. S. Wang, L. Wei, R. S. Shiao, J. Y. Chi, B. V. Volovik, A. F. Tsatsul'nikov, and V. M. Ustinov, J. Vac. Sci. Technol. B **20**, 1158 (2002).
[17] S. Z. Wang, S. F. Yoon, and W. K. Loke, J. Appl. Phys. **94**, 2662 (2003).
[18] TRIM code, available at www.srim.org.
[19] G. Amsel, J. P. Nadai, E. d'Artemare, D. David, E. Girard, and J. Moulin, Nucl. Instrum. Methods **92**, 481 (1971).
[20] R. A. Stall, C. E. C. Wood, P. D. Kirchner, and L. F. Eastman, Electron. Lett. **16**, 171 (1980).
[21] H. A. McKay, R. M. Feenstra, T. Schmidtling, and U. W. Pohl, Appl. Phys. Lett. **78**, 82 (2001).
[22] Y.-C. Chang and D. E. Aspnes, Phys. Rev. B **41**, 12002 (1990).
[23] H. H. Farrell, M. C. Tamargo, J. L. de Miguel, F. S. Turco, D. M. Hwang, and R. E. Nahory, J. Appl. Phys. **69**, 7021 (1991).
[24] W. G. Schmidt, Appl. Phys. A: Mater. Sci. Process. **75**, 89 (2002).
[25] R. J. Hauenstein, D. A. Collins, X. P. Cai, M. L. O'Steen, and T. C. McGill, Appl. Phys. Lett. **66**, 2861 (1995).
[26] C. Calmes, D. Bouchier, D. Debarre, V. Le Thanh, and C. Clerc, Thin Solid Films **428**, 150 (2003).
[27] P. Krispin, V. Gambin, J. S. Harris, and K. H. Ploog, J. Appl. Phys. **93**, 6095 (2003).